ELSEVIER

Available online at www.sciencedirect.com
SCIENCE DIRECT

Journal of Crystal Growth 248 (2003) 249–253

JOURNAL OF CRYSTAL GROWTH

www.elsevier.com/locate/jcrysgro

RDS characterization of GaAsSb and GaSb grown by MOVPE

O.J. Pitts*, S.P. Watkins, C.X. Wang

Department of Physics, Simon Fraser University, 8888 University Drive, Burnaby, BC, Canada V5A 1S6

Abstract

MOVPE-grown n- and p-type (0 0 1) GaAsSb and GaSb were studied using in situ reflectance-difference spectroscopy (RDS), high-resolution X-ray diffraction and Hall measurements. We report RD spectra at 550°C and at room temperature, and the effects of different growth interruptions on GaAsSb RD spectra. The spectra show a strong bulk-related feature, with a maximum at 3.9 eV (GaAsSb) and 3.7 eV (GaSb), at room temperature. GaAsSb and GaSb exhibit a linear electro-optic (LEO) effect. In both n- and p-type materials, the LEO effect results in features in the room temperature RD spectra at the energies corresponding to the E_1 and $E_1 + \Delta_1$ critical points in the bulk band structure.
© 2002 Elsevier Science B.V. All rights reserved.

PACS: 81.05.Ea; 81.15.Gh; 78.40.Fy; 78.20.Jq

Keywords: A1. Optical spectroscopy; A1. Doping; A3. Metalorganic vapor phase epitaxy; B1. Antimonides; B2. Semiconducting III–V materials

1. Introduction

GaAsSb grown on InP is a promising material for optoelectronic and electronic applications. InP/GaAsSb/InP double heterojunction bipolar transistors have achieved cutoff frequencies up to 305 GHz [1]. We have previously reported several aspects of p-type transport and carbon incorporation in GaAsSb using CCl_4 and CBr_4 as carbon precursors [2]. That work was carried out in a horizontal reactor, which did not allow in situ optical measurements. To our knowledge, reflectance-difference spectroscopy (RDS) data have not been reported previously for GaAsSb. Spectroscopic ellipsometry results have been reported for $GaAs_{1-x}Sb_x$ in the composition range $0.22 \leqslant x \leqslant 0.65$ [3]. For GaSb, an RD spectrum has been reported for a p-type sample prepared by Sb decapping [4], but the effect of the type and magnitude of carrier concentration has not been studied previously.

In this work, we present in situ RDS data for the GaAsSb (0 0 1) surface, both at the growth temperature and for as-grown samples at room temperature. We report the effect of growth interruptions on the reflectance anisotropy, with either of the two group V precursors supplied to the surface. Such interruptions can be used, for example, to produce GaAs or GaSb-like interfaces in heterojunction growth. The excess incorporation of As and Sb, respectively, at the surfaces where growth is interrupted, is quantified using

*Corresponding author. Fax: + 604-291-3592.
E-mail addresses: ojpitts@sfu.ca (O.J. Pitts), simonw@sfu.ca (S.P. Watkins).

0022-0248/03/$ - see front matter © 2002 Elsevier Science B.V. All rights reserved.
PII: S0022-0248(02)01892-4

high-resolution X-ray diffraction (XRD). We determine the existence of a surface electric field in n- and p-type GaAsSb and GaSb samples through the identification of a linear electro-optic (LEO) effect in the room-temperature RD spectra.

2. Experiment

The samples were grown by metalorganic vapour phase epitaxy (MOVPE) in a vertical reactor. GaAsSb was grown on InP:Fe (0 0 1) substrates at 550°C. The precursor compounds were triethylgallium (TEGa), trimethylantimony (TMSb), and tertiarybutylarsine (TBAs), with tertiarybutylphosphine (TBP) used during pre-growth annealing of the substrates. The samples were cooled with TMSb supplied to the growth chamber in order to obtain room-temperature RD spectra of the GaAsSb surface. Growth details for GaSb are reported elsewhere [5]. The structural properties of all samples were characterized by XRD, using a Cu anode source and a Bede D3 triple-axis diffractometer. Hall measurements were performed at room temperature in a 0.5 T magnetic field, using the standard Van der Pauw geometry. RDS measurements were performed in the standard way, with the RDS signal defined as the real part of the complex reflectance anisotropy [6]. For a set of nonintentionally doped samples, growth was periodically interrupted under a flux of TBAs and TMSb, respectively. Multitransient spectroscopy [7] was performed for these growths in order to construct time-resolved RD spectra with a temporal resolution of 0.25 s.

3. Results and discussion

The RD spectra of the GaAsSb surface at 550°C under different precursor flow conditions were obtained from the time-resolved data set. Representative spectra are shown in Fig. 1. Curve (a) is the RD spectrum for growing GaAsSb, curve (b) is the RD spectrum after a 10 s growth interruption (GRI) under TBAs flux, and curve (c) is the RD spectrum after a 50 s GRI under TMSb flux. For both curves (b) and (c), the growing GaAsSb spectrum is shown as a dotted line for comparison. The main features of the three spectra are qualitatively similar; a broad negative feature at low energy and a stronger positive feature at high energy. The spectra bear a strong resemblance to the RD spectrum of (0 0 1) GaAs contaminated with residual Sb [8]. The low-energy feature does not show a clear minimum for growing GaAsSb. Under TBAs exposure, a minimum is observed at 2.8 eV and the positive feature shifts to 4.0 eV. Under TMSb flux, on the other hand, the negative feature becomes stronger and is centred around 2.3 eV whereas the high-energy peak exhibits a smaller shift, to 3.8 eV.

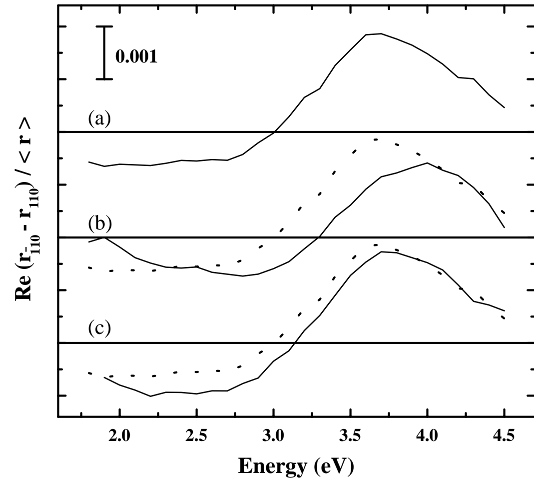

Fig. 1. RD spectra of the GaAsSb (0 0 1) surface at 550°C: (a) growing GaAsSb, (b) after 10 s under TBAs, and (c) after 50 s under TMSb. Dotted lines show the growing GaAsSb spectrum.

The time dependence of the change in the RD spectrum is quite different under TBAs and TMSb exposure. In the case of TBAs exposure, the spectrum changes from the GaAsSb growth spectrum (Fig. 1 a) to the stabilized spectrum (Fig. 1 b) within 3 s, and exhibits no further change upon continued TBAs exposure. For TMSb flux, on the other hand, the spectrum evolves slowly throughout the 50 s GRI and is not stabilized, even at the end of this time period. This difference in the rate of change is similar to that seen on GaAs (0 0 1) surfaces alternately exposed to TBAs and TMSb [9].

X-ray diffraction data were obtained from two nonintentionally doped samples with ten GRIs separating 32 s GaAsSb growth steps. Fig. 2(a) shows the experimental rocking curve about the InP (0 0 4) reflection for the sample with 10 s GRIs under TBAs flux, as well as a simulated curve calculated from dynamical diffraction theory using the Bede RADS software package. Fig. 2(b) shows the data and simulation for the sample with 50 s GRIs under TMSb flux. The positions of the superlattice satellite peaks do not independently determine the average GaAsSb composition and the amount of As or Sb incorporated during the GRIs, but an approximate estimate can be obtained by fitting the intensities of the simulated peaks to the data. To calculate the simulated diffraction patterns, the As and Sb-rich layers were approximated by thin layers of either GaAs or GaSb between uniform layers of GaAsSb. For the TBAs GRI sample, the best fit simulation was obtained with ten periods of 116 Å GaAsSb, with a Sb mole fraction of 0.497, separated by 7.6 Å GaAs. For the TMSb sample, the best fit simulation used ten periods of 118 Å GaAsSb, with a Sb mole fraction of 0.462, separated by 2.5 Å GaSb.

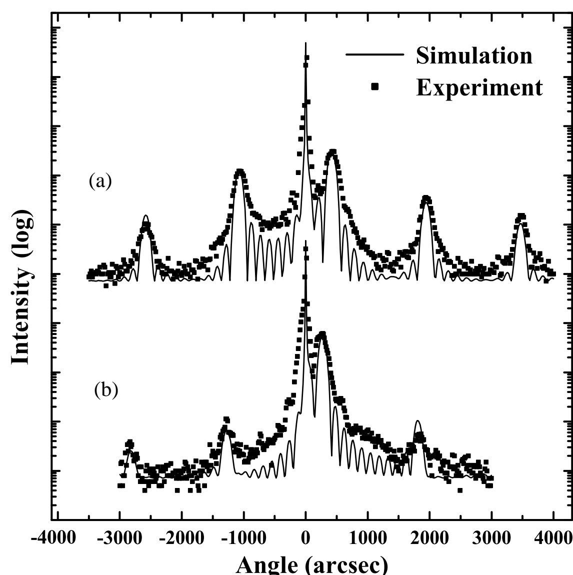

Fig. 2. XRD rocking curves (data and simulations) about the InP (0 0 4) reflection for GaAsSb exposed periodically to (a) TBAs and (b) TMSb.

Thus, the 10 s TBAs GRI results in approximately one monolayer (ML) of excess As incorporation, whereas the 50 s TMSb GRI results in approximately 0.4 ML excess Sb incorporation.

GaAsSb samples, nominally 1100 Å thick, were grown without GRIs to study the effects of n- and p-type doping. The electrical and structural properties of the samples, obtained from Hall and XRD measurements, are summarized in Table 1. Sample A is n-type GaAsSb doped with 8.9×10^{-7} mol/min of H_2S, sample B is nonintentionally doped, and samples C and D are p-type GaAsSb doped with CBr_4 flows of 1.9×10^{-8} and 1.9×10^{-7} mol/min, respectively. All samples were grown with identical TEGa, TMSb and TBAs flows; the lower growth rate and more As-rich composition of the heavily carbon-doped sample D are consistent with trends documented previously [2]. Fig. 3 shows the RD spectra of GaAsSb samples A–D, at room temperature. The spectra were obtained in situ before exposure of the samples to atmospheric oxygen. A strong positive feature is observed, as in the elevated temperature spectra. At room temperature, the maximum is at 3.9 eV, which correlates with a peak in the pseudodielectric function of GaAsSb [3], and can be attributed to a surface-modified bulk transition. The energies of the E_1 and $E_1 + \Delta_1$ critical points for the relevant alloy composition, from ellipsometric data [3], are indicated by arrows for each RD spectrum. The features in the reflectance anisotropy around these transitions are due to an LEO effect produced by the surface electric field. This effect has been studied previously on GaAs (0 0 1) [10] and GaSb (0 0 1) [4] surfaces. The LEO features are superimposed on a broad negative region for the unoxidized as-grown

Table 1
Thickness (z), Sb mole fraction (x), carrier concentration (n or p), and Hall mobility (μ_H) of GaAsSb samples A–D

Sample	Dopant	z (Å)	x	n or p (cm^{-3})	μ_H (cm^2/V s)
A	H_2S	1100	0.51	n-type, 1.6×10^{18}	990
B	none	1150	0.53	p-type, 4.5×10^{16}	60
C	CBr_4	1100	0.50	p-type, 1.6×10^{18}	42
D	CBr_4	1000	0.43	p-type, 1.2×10^{19}	35

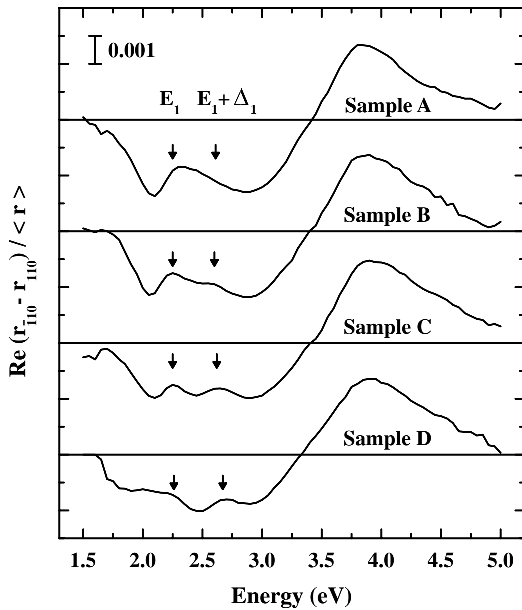

Fig. 3. RD spectra of n- and p-type GaAsSb samples at room temperature. The details of the samples are given in Table 1.

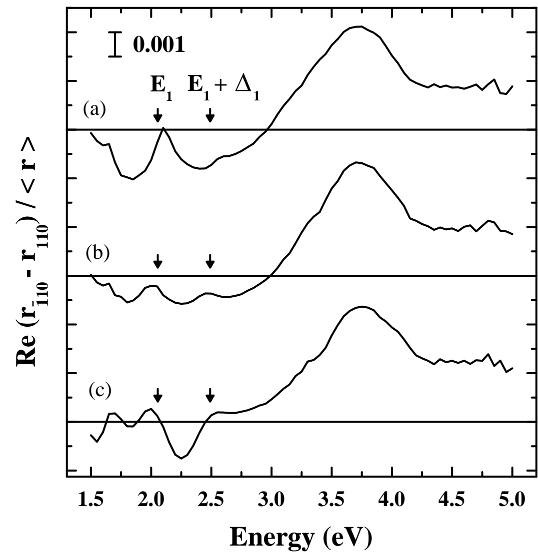

Fig. 4. Room-temperature RD spectra of (a) Te-doped GaSb substrate, (b) undoped GaSb substrate, and (c) C-doped GaSb epilayer.

samples. Upon exposure to air, the overall negative anisotropy in this region disappears, with only the LEO features remaining (data not shown). The broad negative feature is therefore related to surface structure.

The RD spectrum for sample A (n-type) shows a positive feature near the E_1 energy (2.25 eV), without clearly resolved peaks for the E_1 and $E_1 + \Delta_1$ transitions. For the p-type samples, positive features appear at the E_1 and $E_1 + \Delta_1$ energies, their amplitude increasing with the hole concentration. The amplitude of the negative feature at 2.1 eV decreases with increasing hole concentration, while the signal at 2.5 eV becomes more negative, forming a clear valley between the E_1 and $E_1 + \Delta_1$ peaks for the carbon-doped samples. The dependence of the LEO features on the carrier concentration appears to be different from that observed in GaAs [11], but the fact that these features change with the type and level of doping indicates that they are surface electric field-related.

The RD spectra shown in Fig. 4(a) and (b) were obtained from a Te-doped ($n = 1 \times 10^{18}\,\text{cm}^{-3}$) and undoped ($p = 1.5 \times 10^{17}\,\text{cm}^{-3}$) GaSb substrate, respectively. The substrates were heated under TMSb to remove the surface oxide, then cooled to room temperature. Fig. 4(c) shows the room-temperature RD spectrum of a carbon-doped GaSb epilayer, with a hole concentration $p = 9 \times 10^{18}\,\text{cm}^{-3}$. The energies of the E_1 and $E_1 + \Delta_1$ critical points [12] are indicated by arrows for each RD spectrum. The spectra are similar to a previously reported RD spectrum obtained by thermal Sb decapping of a p-type GaSb sample, which exhibited a $c(2 \times 6)$ reconstruction [4].

Apart from the LEO signal, the main features of the GaSb RD spectrum are a maximum[1] at 3.8 eV, and a broad, slightly negative region from 1.5 to 3 eV. The peak at 3.8 eV correlates with a peak in the pseudodielectric function of GaSb [12], and is therefore bulk related. The dependence of the LEO line shape on the carrier type and concentration is qualitatively similar to the behaviour in GaAsSb. The n-type sample shows a sharp positive peak 50 meV above the E_1 energy, a weak positive

[1] The previously reported spectrum used the opposite sign convention for the reflectance anisotropy, so that the 3.8 eV feature appeared as a minimum.

shoulder about 100 meV above the $E_1 + \Delta_1$ energy, and a negative feature at 1.8 eV. For both the undoped substrate and the carbon-doped epilayer, positive features are located 50 meV below the E_1 energy, and close to the $E_1 + \Delta_1$ energy. Both features are thus red shifted by 100 meV with respect to the RD features of the n-type sample. In contrast, such a shift is not evident in Fig. 3, but it may be obscured by the broader line shapes in the GaAsSb data. The magnitude of the negative feature at 1.8 eV decreases with increasing hole concentration, whereas the negative feature between the E_1 and $E_1 + \Delta_1$ energies becomes stronger.

4. Conclusions

We have reported the RD spectra for GaAsSb on InP under conditions of MOVPE growth, and growth interruptions with either TMSb or TBAs exposure. The spectra show a broad negative region at low energy and a strong positive feature near 3.7 eV, which blue shifts by 100 and 300 meV under TMSb and TBAs, respectively. No distinct dimer-related features were identified. Growth interruptions under TMSb and TBAs result in excess incorporation of Sb and As, respectively. The incorporation of As and the evolution of the RD spectrum under TBAs exposure are both considerably faster than the corresponding processes under TMSb exposure. RD spectra at room temperature, of n- and p-type GaAsSb and GaSb, show a bulk-related positive feature at 3.9 and 3.7 eV, respectively. Both materials exhibit features at the energies corresponding to the E_1 and $E_1 + \Delta_1$ critical points, which are due to the LEO effect associated with the surface electric field.

Acknowledgements

This work was supported by the Natural Sciences and Engineering Research Council of Canada (NSERC).

References

[1] C.R. Bolognesi, M.W. Dvorak, N. Matine, O.J. Pitts, S.P. Watkins, Japan. J. Appl. Phys. 41 (2002) 1131.
[2] S.P. Watkins, O.J. Pitts, C. Dale, X.G. Xu, M.W. Dvorak, N. Matine, C.R. Bolognesi, J. Crystal Growth 221 (2000) 59.
[3] D. Serries, M. Peter, N. Herres, K. Winkler, J. Wagner, J. Appl. Phys. 87 (2000) 8522.
[4] C. Goletti, U. Resch-Esser, J. Foeller, N. Esser, W. Richter, B. Brar, H. Kroemer, Surf. Sci. 352–354 (1996) 771.
[5] R. Wiersma, J.A.H. Stotz, O.J. Pitts, C.X. Wang, M.L.W. Thewalt, S.P. Watkins, J. Electron. Mater. 30 (2001) 1429.
[6] I. Kamiya, D.E. Aspnes, L.T. Florez, J.P. Harbison, Phys. Rev. B 46 (1992) 15894.
[7] D.E. Aspnes, I. Kamiya, H. Tanaka, R. Bhat, J. Vac. Sci. Technol. B 10 (4) (1992) 1725.
[8] O.J. Pitts, S.P. Watkins, C.X. Wang, J.A.H. Stotz, M.L.W. Thewalt, J. Electron. Mater. 30 (2001) 1412.
[9] O.J. Pitts, S.P. Watkins, C.X. Wang, V. Fink, K.L. Kavanagh, submitted to Phys. Rev. B.
[10] S.E. Acosta-Ortiz, A. Lastras-Martinez, Phys. Rev. B 40 (1989) 1426.
[11] H. Tanaka, E. Colas, I. Kamiya, D.E. Aspnes, R. Bhat, Appl. Phys. Lett. 59 (1991) 3443.
[12] S. Zollner, M. Garriga, J. Humlíček, S. Gopalan, M. Cardona, Phys. Rev. B 43 (5) (1991) 4349.